UCL

UNIVERSITY COLLEGE LONDON

DEPARTMENT OF PHYSICS AND ASTRONOMY

Ganymede: Mighty Little Magnetic Moon

Research Essay

Author: Alexandre Santos
Supervisors: Nicholas Achilleos and Dimitrios Millas

MSc Astrophysics

24th March 2022

Contents

List of Figures

List of Tables

Chapter 1

Introduction

Throughout our solar system, we see a large diversity in the characteristics of its composing bodies, from our host star, the Sun, to the asteroids and comets that make up the Oort cloud at the edges of our solar system. One important feature of some of them is the presence of a magnetic field that surrounds the body. In most cases, this magnetic field is generated deep within their core, where rapidly rotating hot metal generates strong convective currents that, in turn, give rise to the observable dipole magnetic field that permeates the space around the object, called its magnetosphere. However, and as we will see, there exist other ways a planetary body can acquire a magnetic field that do not impose such constrains on its core's composition, requiring instead the presence of an ambient magnetic field and material with conductive properties in the object's interior. As such, the different magnetic fields generated by a given celestial body can be used as a powerful tool to study its inner composition.

In this report, we will focus on how one can use magnetic field measurements to probe the interior of planets and moons, with a special emphasis on Ganymede, the primary scientific target of the upcoming European Space Agency's JUICE mission, set to launch in 2023. In order to do that, we will begin with a description of the magnetospheres of the Jovian system and some external factors that might impact the behaviour of the total magnetic field of the system. We then present some of the currently used methods to relate magnetic field measurements, taken during flybys or in orbit, with constraints on the inner composition of planetary bodies, mostly focusing on the study of Europa, Callisto and Ganymede, as they might possess a subsurface ocean layer capable of harbouring life. Lastly, we introduce the JUICE mission, its scientific objectives and how we can use its magnetometer to study the total magnetic field felt at different locations within the Jovian system, infer the properties of the inner composition of Europa, Callisto and Ganymede, and analyse the possibility of using its data to detect variations in Jupiter's magnetosphere due to its interaction with solar wind.

1.1 Magnetospheres in our solar system

In our solar system, we have detected evidence of an intrinsic magnetic field in most major planets such as Mercury, Earth, Jupiter, Saturn, Uranus and Neptune, as well as the Sun. More recently, the Galileo flybys provided us with evidence for a magnetosphere around Ganymede [1], one of the moons of Jupiter, the largest in our solar system and the main focus of our work. In this section we will introduce the main characteristics of the Sun's own magnetosphere, the heliosphere, which can heavily impact every other planetary magnetosphere in our solar system, and the magnetospheres present within the Jovian

system.

1.1.1 The heliosphere

The solar magnetosphere constitutes one of the largest and most complex structures in our solar system. It is much larger than any planetary magnetosphere, and extends far beyond any planet's orbit. In terms of structure, it shows significant differences from a regular planetary magnetosphere, mostly due to constant interactions with the surrounding interstellar medium (ISM). The frontier between the heliosphere and the ISM is called the heliopause, and it's in this region where the solar generated particle flow equalises its pressure with the ISM's. The heliosheath, which is thought to be around 94 AU away from the Sun [2], corresponds to an intermediate region, between the terminal shock region, where the plasma flow changes from supersonic to subsonic, and the heliopause. Finally, its interaction with incoming cosmic rays from the ISM also generates a prolonged tail of charged particle flow, called the heliotail, as the Sun moves across space (**Figure 1.1**).

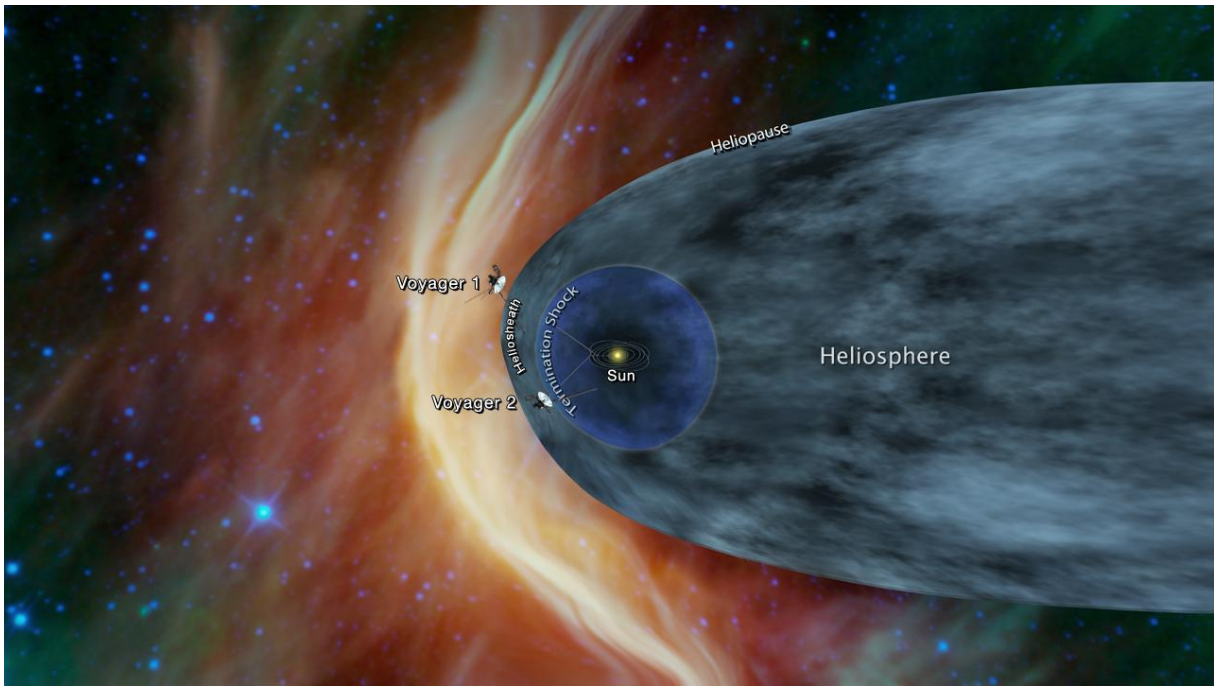

Figure 1.1: Schematic representation of the heliosphere and estimated location of the Voyager 1 and 2 spacecrafts [3].

It has been shown that the release of charged particles or plasma from different parts of the Sun's atmosphere is heavily correlated with the solar activity. Upon release, these charged particles follow the magnetic field lines and are accelerated, reaching supersonic speeds at a distance $r = r_c$, named the critical point. From there, its speed approaches an asymptotic value, which varies depending on the temperature of the plasma (**Figure 1.2**). The solar wind model developed by Parker [4][5] shows that the critical point is achieved at around 10 solar radii, which is much closer than the average distance of Mercury to the Sun. As such, the plasma flow travels almost all of its journey across the solar system at supersonic speeds. However, in order for the plasma flow pressure to equalise the ISM's near the heliopause, it must then decelerate, reaching subsonic speeds at the so called termination shock region. The plasma then eventually crosses the heliopause, exiting the heliosphere into the interstellar medium. This flow of charge particles is normally

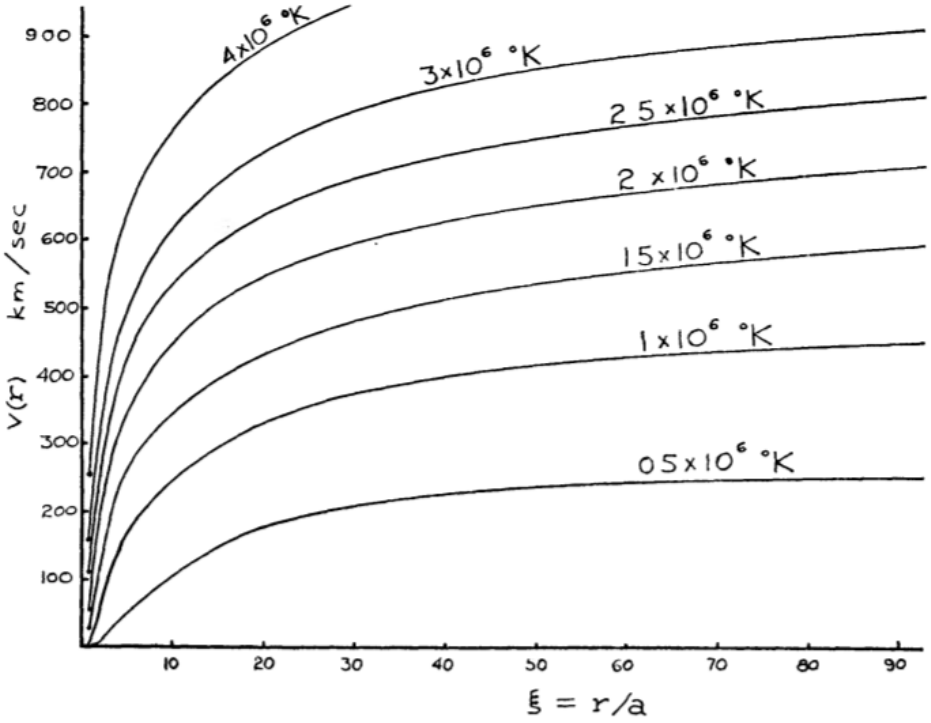

Figure 1.2: Spherically symmetric hydrodynamic expansion velocity $v(r)$ of an isothermal solar corona with temperature T_0 plotted as a function of r/a, where a is the radius of the corona and has been taken to be 10×10^{11} cm [4].

called solar wind, while massive ejections of hot plasma from the Sun's corona are called coronal mass ejections (CME), which typically are associated with solar flares observed at the Sun's surface. Both of these effects can heavily impact the magnetospheres of other bodies in the system. One of the possible effects is the slow removal of a planet's atmosphere due to the interaction with the incoming high energy particles, where some of their energy is transferred to the particles that constitute the upper layers of the planet's atmosphere. This process, called sputtering, is thought to be one the main causes for atmospheric loss in planets such as Mercury and Mars, as found by the MAVEN mission [6].

Over the years, a variety of space missions allowed us to gain a better understanding of the Sun's magnetosphere, but many questions still remain unanswered. Both Voyager 1 and 2, as well as some other ground-based observation missions, have revolutionised our understanding of the heliosphere and how the solar plasma flow propagates across our system. The outer edges of the heliosphere proved particularly intriguing, as Voyager measurements showed no evidence for acceleration of anomalous cosmic rays at this region, despite being predicted for over 25 years [7]. The heliosphere also proved to be far more dynamic than previously thought, as measurements for the energies of particle and plasma flows taken by Voyager 1 and 2 showed radically different underlying differences in the magnetic structure. As this flow of charged particles can heavily impact both a planet's magnetosphere and atmosphere, it is crucial we develop a solid understanding on how they propagate across the system as well as how they are generated. In our work, we will focus mainly on how solar winds and CMEs can change Jupiter's magnetosphere and how we can detect these changes.

1.1.2 Magnetospheres in the Jovian system

This essay will focus mainly on the magnetospheres present in the Jovian system, which include the magnetospheres of Jupiter and Ganymede, and how we can use magnetic field measurements to extract a variety of properties of both the dynamics of the magnetic environment of this system, as well as set constrains on the interior composition of its moons. In order to do so, we will begin by introducing the principal features of these two magnetospheres.

1.1.2.1 Jupiter's magnetosphere

Just like Earth, Jupiter possesses a magnetic field produced by electric currents generated at the planet's core. However, Jupiter's magnetosphere is far more complex and dynamic than Earth's, having a magnetic moment of around $2.83 \times 10^{20}\,\mathrm{T\,m^3}$, tilted by 10 ° in relation to its rotational axis. This results in a magnetic field with equatorial strength of 420 000 nT, which is around 20 times greater than the average field strength of Earth. Its overall shape is also quite different, as Jupiter possesses an enormous toroidal structure composed of relatively cool plasma, extending from $5 - 10\,R_J$. This structure is composed of charged particles originated primarily from volcanic eruptions in Io, another of Jupiter's moons, which expel sulphur and oxygen ions into space. These particles accumulate near Io's orbit, becoming trapped in the so called "Io plasma torus", which co-rotates with Jupiter (**Figure 1.3**). Despite the continuous inflow of plasma into the torus, there is also a slow and progressive outflow of these charge particles, as they are radially transported outward from the torus due to a variety of processes, as explained in [8]. It is estimated that Io experiences a total mass loss of one ton per second, in order to maintain this structure [9]. Although we will not consider the impact of this structure in our work, it fundamentally changes the overall behaviour of Jupiter's magnetosphere at those distances and its interaction with Jupiter and some of its moons produces a variety of fascinating effects, such is the case of Jupiter's aurorae. More information about these interactions is described in [9].

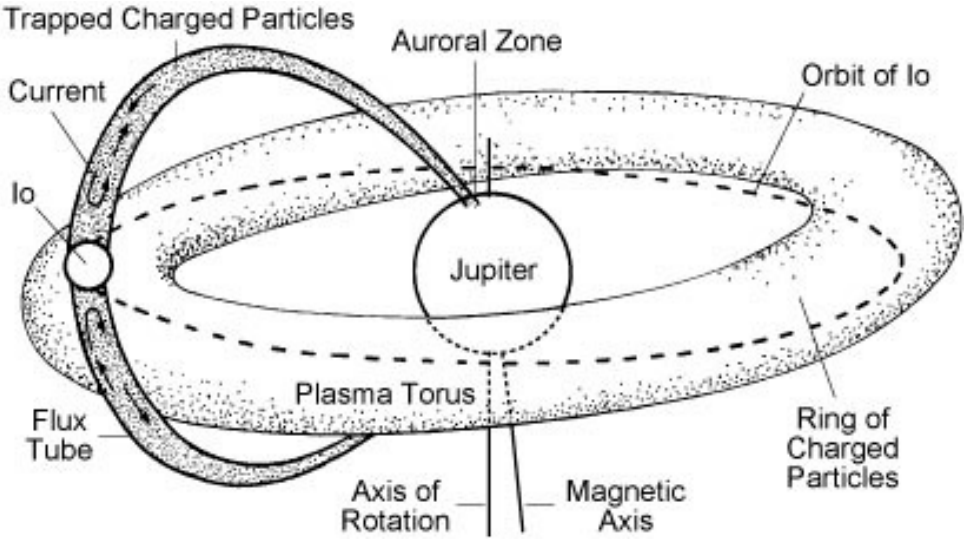

Figure 1.3: Schematic representation of the Io torus [10].

Moving further out into the middle magnetosphere, which ranges from $\sim 10 - 40\,R_J$, we observe yet another contrasting feature, where due to a combination of a very strong

centrifugal force caused by Jupiter's rapid rotation, a plasma pressure gradient and Lorentz force, we observe a flattening of the magnetic field lines creating a disk-like structure that lies close to the dipole's equator, thus tilted in relation to Jupiter's rotational axis [8]. It is in this region where we begin to see a clear departure from a Jupiter co-rotational motion of the plasma, as the planets intrinsic magnetic field is significantly weaker at these distances. As such, strong electrical currents form within the disk, generating a significant magnetic moment, comparable to that planet's own internal field. This added contribution results in a further radial expansion of the typical magnetosphere structure associated with a dipole magnetic field, creating the so called magnetodisk.

Solar winds and coronal mass ejection events can also heavily impact the overarching magnetic field felt across the Jovian system. This is mainly due to the added pressure exerted on Jupiter's magnetosphere by the incoming charged particles of the solar wind. As such, its solar-facing side tends to compress, while the rest of the magnetosphere tends to get stretched out by the interaction with the incoming plasma flow (**Figure 1.4**). The magnetopause is defined by the balance of the dynamic pressure of the solar wind, magnetic pressure and thermal plasma pressure and so, since the solar wind pressure will be lower in the night-side, the magnetopause will be able to extend further out in this region. The so called Vasyliunas cycle [11] further contributes to this effect, where plasma tubes originated by the Jupiter-Io interaction, and generally radially restrained by the day-side solar wind dynamic pressure, expand as they rotate to the night-side [12]. This radial expansion occurs as the plasma pressure becomes comparable to the field pressure and leads to the loss of large quantities of plasma through the magnetotail. The flux tubes are then once again mass-loaded as they rotate towards the day-side, restarting the cycle. This cycle occurs for plasma which is on closed field lines and predominantly in the equatorial region. The Dungey cycle, however, occurs on field lines that, due to the interaction with the solar wind, open out and get stretched towards the night-side, dragging plasma downstream in order to help form the distant magnetotail [12].

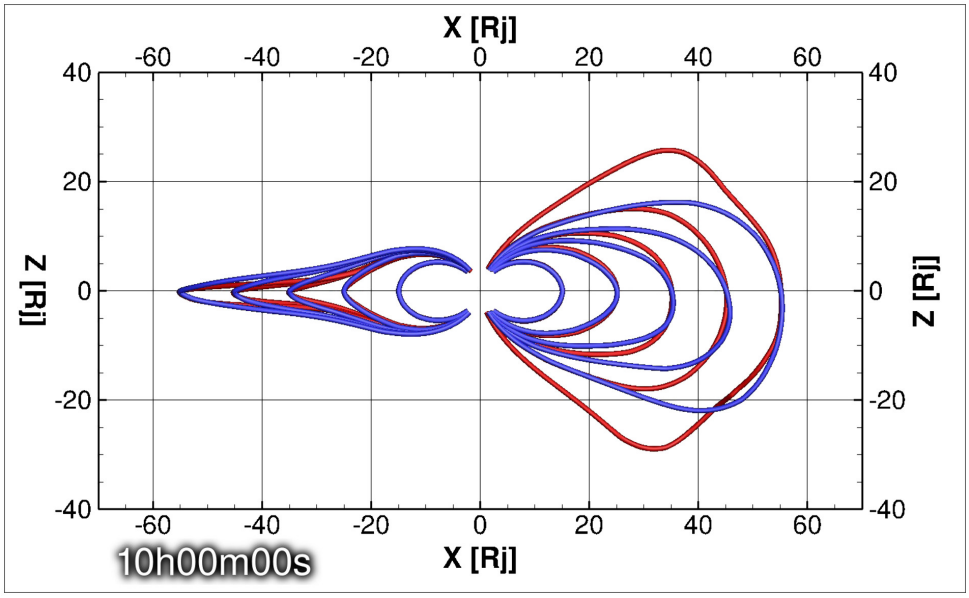

Figure 1.4: Magnetic field lines for quiet solar wind conditions (in blue) and for very disturbed solar wind conditions (in red), 10 h after the high-density solar wind reached the magnetosphere in the noon-midnight meridian (side view). The solar wind comes from the right [13].

Due to the nominal plasma flow corotating with Jupiter, we can expect some asymmetry in the resulting flow, as the incoming solar wind would help accelerate the plasma flowing

in solar wind direction and decelerate the one flowing opposite to it. An example of such a scenario is shown in **Figure 1.5**. Several simulation models have been made in order to study these interactions, where one tries to predict the resulting plasma flow change due to the incoming solar wind, for different speeds and plasma density [14][13]. Of particular interest are the changes in plasma flow currents near the equatorial plane, as they can experience the highest amount of acceleration/deceleration due to this effect. As we will discuss further on, in our work we assess the possibility of using in situ magnetic field data to detect and study these variations in Jupiter's magnetosphere, thus helping set constrains on the expected behaviour given by current computational models of this effect.

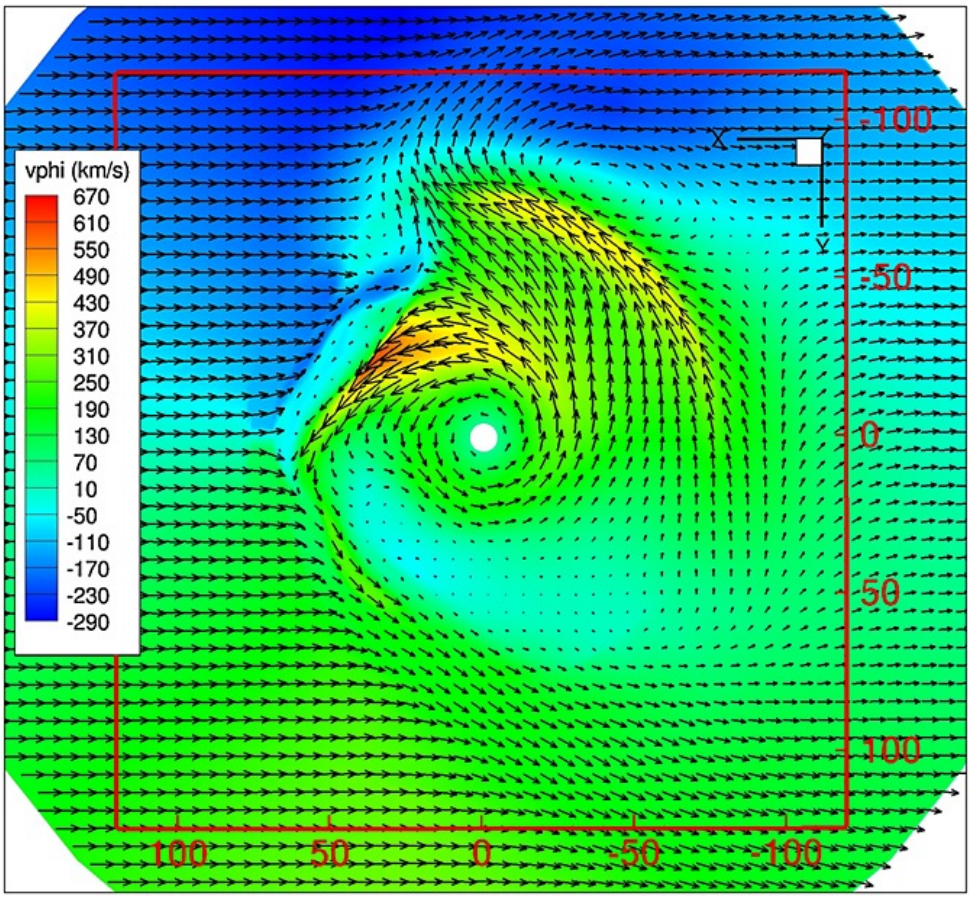

Figure 1.5: Velocity in the equatorial plane (top view). The black arrows represent the velocity in this plane; the colour contours the azimuthal velocity. The solar wind comes from the left [14]

1.1.2.2 The small magnetosphere of Ganymede

Ganymede is the only intrinsically magnetised moon in the Solar System, possessing a permanent magnetic moment that in turn generates a dipole field with an equatorial field strength of 719 nT and 1440 nT at the poles. While Ganymede's intrinsic magnetic field is much smaller than the one produced by Jupiter, but it is still strong enough to create a small magnetosphere carved deep within Jupiter's, with a radius of $r \approx 5$ Ganymede radii (R_G). As such, we are able to observe closed field lines near the equator, while in the polar regions we see open field lines following Jupiter's overall magnetic line distribution. Measurements have shown that Ganymede's magnetic moment is tilted around 176° with respects to its rotational axis [1], pointing in an opposite direction to Jupiter's magnetic moment and so, in the equatorial regions, magnetic reconnection can occur at $\sim 2-3$ Ganymede radii from its centre. This process corresponds to a merge of the magnetic

field lines coming from Jupiter and Ganymede. In fact, we have observed this effect when analysing the interaction between Earth's own magnetosphere with strong solar winds or coronal mass ejection events [15], but due to the sporadic nature of such events, the impact of magnetic reconnection in the overall plasma flow and the timescales involved have not yet been fully understood. One of the main open questions is the transient period between the original and the post-reconnection configuration of the magnetosphere. Since this mechanism in the Jupiter-Ganymede system is solely caused by the interaction between these two magnetospheres, magnetic reconnection events are continuously occurring, as Ganymede rotates around Jupiter, providing us with a far more consistent environment in which to study this interaction.

1.2 Using magnetic field measurements to probe the internal composition of Jovian moons

The study of the magnetic field that surrounds a planetary body can serve as a powerful tool to determine, not only the properties of the local space environment, but also key properties of its internal composition. The magnetospheres of gas giants, such as Jupiter, are of particular interest as they present noticeable changes due to interactions with its large moons. These changes in the overarching magnetic field are mostly felt close to the moons' surface, but in some cases can assume a dominant role in the total magnetic field at these distances. As such, several missions are being developed with the goal of better understanding these complex systems. In this essay we will present some examples on how magnetic field measurements are being used to indirectly probe possible subsurface ocean layers in some Jovian moons.

1.2.1 Magnetic field contributions in the Jovian system

In order to detect and interpret the changes in the total magnetic field caused by the interaction of Jupiter's moons with its own magnetic field, one must first develop a comprehensive model of the different magnetic field contributions. As seen previously, the most important contributions correspond to the intrinsic magnetic fields present in the system. These can, for most cases, be easily described as a dipole magnetic field generated by a constant magnetic moment. This magnetic moment is generally not aligned with the planet or moon's rotational axis, thus resulting in the poles not necessarily corresponding to the magnetic poles of the magnetic field. As we will mostly focus on the Jupiter-Ganymede system, where the magnetic moments are tilted about $10\,^\circ$ and $176\,^\circ$, respectively, the magnetic poles are not very different from their rotational poles. However, this small difference is important, as it can originate an induced field response in some of Jupiter's moons, as observed in [16][1].

This induced magnetic field is thought to be generated due to the interaction of Jupiter's rotating magnetic field and conductive material in a moon's interior via Faraday's law. As such, the time-varying magnetic field of Jupiter results in the creation of electric currents in the conductive material, that in turn generate an induced dipole magnetic field. The strength of this induced field is thus highly dependent on the conductive properties of the moon's interior. As we will see, there is evidence for a significant induced response in several moons of Jupiter such as Europa, Callisto and Ganymede [16][1]. There are, however, several other contributions one should take into account when constructing a detailed model of the over, such as the added contribution of Jupiter's magnetodisk field

and the impact of solar wind and coronal mass ejection events. In our work we will try to incorporate some of these contributions in order to provide the best possible predictions for the actual behaviour of the magnetic environment of the system.

1.2.2 Europa and Callisto

Europa and Callisto are two of the four Galilean moons, along with Ganymede and Io. These moons possess very tenuous atmospheres composed essentially of oxygen and carbon dioxide, respectively, with very low surface pressure at around 0.1 and 0.75 µPa and low surface temperatures of about 102 and 134 K. While Callisto's surface is also composed of rocky material, both moons have large quantities of ices spread across their surface. Measurements have shown that, in both cases, a significant portion of these ice masses are composed of water ice [17]. This icy layer is especially apparent for the case of Europa, giving the moon a characteristically smooth look.

The Galileo spacecraft was able to study some of the properties of these moons, such as the composition of the moons' surface and atmosphere and the total magnetic field. These measurements were taken during several flybys of both Europa and Callisto, and showed evidence of an induced magnetic field generated in both of these moons, with a response similar to the one given by a perfectly conducting spheres. This behaviour is quite different to the one predicted assuming an icy and rocky interior for the moons, as it would lack the necessary conductivity to generate such a response. It would, in fact, require a globally distributed highly conductive medium located close to the surface [16]. The presence of liquid water at the surface is highly unlikely, as the temperature of these moons is too low for water to exist in liquid form. It is then believed that the explanation for this behaviour is the existence of a salty subsurface ocean layer, just a few kilometers below the surface, where the moon's interior provides enough heat for water to exist in liquid form. This hypothesis was later strengthened by the discovery of water vapour coming from possible cryovolcanism in Europa [18], pointing once again towards the presence of liquid water in the moon's interior.

We can then use the measurements taken by Galileo to constrain the properties of this ocean layer, such as its thickness, depth and conductivity. This approach is well documented in [16] and it is the one we will be using in order to model the induced magnetic field response. In [16], the moon's interior was modelled using a shell of uniform conductivity surrounding an insulating core and surrounded by an insulating outer shell (**Figure 1.6**). The response of a perfectly conducting spherical shell with a given width is a classic electromagnetism problem, where using Maxwell's equations and Ohm's law we can obtain the diffusion equation for the magnetic field inside the conducting shell:

$$\nabla^2 \mathbf{B} = \mu\sigma \frac{\partial \mathbf{B}}{\partial t} \tag{1.1}$$

where μ corresponds to the magnetic permeability of the medium and σ to its electrical conductivity. In [16], μ was considered to be equal to the vacuum magnetic permeability μ_0. It is also worth mentioning that the contributions of a displacement current were neglected. As for the insulating regions, given that they will not interact with the time varying magnetic field, we must have:

$$\nabla^2 \mathbf{B} = 0 \tag{1.2}$$

This last equation holds even beyond the moon's surface, where the conductivity is still low, as long as one also neglects the possible contributions of plasma convection effects,

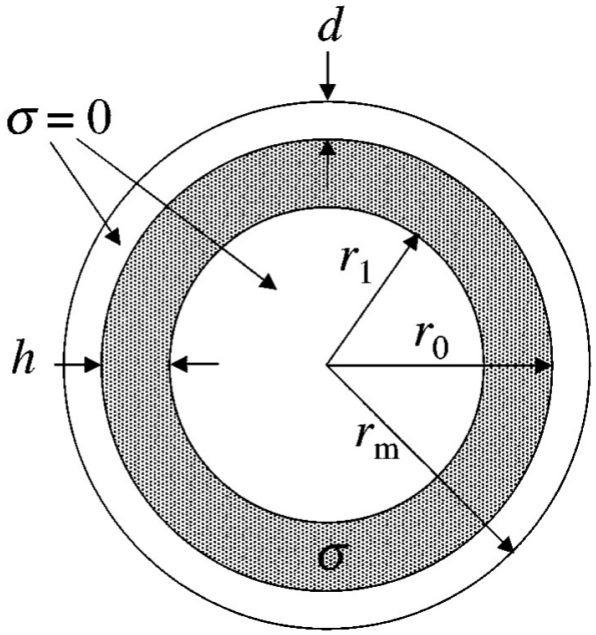

Figure 1.6: Representation of the simple model used to describe the induced magnetic field response, with a conductive shell surrounded by both an insulating core and an insulating outer shell [16].

as stated in [16]. We can then model the primary magnetic field, in this case the time varying magnetic field caused by Jupiter's rotation, as an oscillating field with frequency ω along a specified unit vector $\vec{\mathbf{e}_0}$, expressed by the real part of:

$$\mathbf{B}_{\text{prim}} = B_{\text{prim}}\, e^{-i\omega t}\vec{\mathbf{e}_0} \tag{1.3}$$

In general, this primary field can oscillate with more than one frequency and in more than one direction, but one can always add these other solution components, as the new solution would also satisfy both **Equations 1.1** and **1.2**. As the variations in Jupiter's magnetic field are only felt for distances in the order of $\sim 1R_J$, $\mathbf{B}_{\text{prim}}$ can be considered uniform at a given time in the spatial scale of the moons. The total magnetic field solution, $\mathbf{B}$, must yet also satisfy three boundary conditions:

- The total magnetic field solution must be continuous across the border between the conductive and insulating materials;
- The total magnetic field must be finite at the core, where $\mathbf{r} = 0$;
- The total magnetic field solution must be asymptotically equal to the primary magnetic field, $\mathbf{B}_{\text{prim}}$, when far from the conductive shell, where $|\mathbf{r}| = r \gg r_m$.

Considering that we will also have a secondary magnetic field contribution, $\mathbf{B}_{\text{sec}}$, coming from the induced magnetic field generated within the moon, the total magnetic field will be given by $\mathbf{B} = \mathbf{B}_{\text{prim}} + \mathbf{B}_{\text{sec}}$. Now, since $\mathbf{B}_{\text{prime}}$ is considered to be uniform, we can obtain a solution for the induced magnetic field outside the conductive shell, which will correspond to a dipole field:

$$\mathbf{B}_{\text{sec}} = \frac{\mu_0}{4\pi}\left[3(\mathbf{r}\cdot\mathbf{M})\mathbf{r} - r^2\mathbf{M}\right]/r^5 \tag{1.4}$$

where its magnetic moment $\mathbf{M}$ oscillates along the direction $\vec{\mathbf{e}_0}$ with frequency ω, just like the primary field. As such, the magnetic moment is given by:

$$\mathbf{M} = -\frac{4\pi}{\mu_0} A e^{i\phi} \mathbf{B}_{\text{prim}}\, r_{\text{m}}^3/2 \tag{1.5}$$

Substituting this in **Equations 1.1**, we obtain the following expression for the secondary field contribution:

$$\mathbf{B}_{\text{sec}} = -A e^{-i(\omega t-\phi)} B_{\text{prim}} \left[3\left(\mathbf{r}\cdot\mathbf{e}_0\right)\mathbf{r} - r^2\mathbf{e}_0\right] r_{\text{m}}^2/\left(2r^5\right) \tag{1.6}$$

where the physically induced magnetic field is given by the real part of this expression. As shown in [19], both the normalised amplitude A and phase lag ϕ of the induced response in relation to the primary field are real numbers and given by the equations:

$$A e^{i\phi} = \left(\frac{r_0}{r_{\text{m}}}\right)^3 \frac{R J_{5/2}\left(r_0 k\right) - J_{-5/2}\left(r_0 k\right)}{R J_{1/2}\left(r_0 k\right) - J_{-1/2}\left(r_0 k\right)} \tag{1.7}$$

$$R = \frac{r_1 k J_{-5/2}\left(r_1 k\right)}{3J_{3/2}\left(r_1 k\right) - r_1 k J_{1/2}\left(r_1 k\right)} \tag{1.8}$$

where $k = (1-i)\sqrt{\mu_0\sigma\omega/2}$ is a complex wave vector, J_m is the Bessel function of first kind and order m and r_1, r_0 and r_m are the different radii illustrated in **Figure 1.6**. It is further shown in [16], that we can describe the induced response of the conductive shell with an arbitrary conductivity and size as a function of the induced response produced by a perfectly conducting moon of radius r_m, $\mathbf{B}_{\text{sec},\infty}$, as given by:

$$\mathbf{B}_{\text{sec}} = A e^{i\phi} \mathbf{B}_{\text{sec},\infty} \tag{1.9}$$

and so taking the real part of this solution we get:

$$\mathbf{B}_{\text{sec}}(t) = A\mathbf{B}_{\text{sec},\infty}(t - \phi/\omega) \tag{1.10}$$

which states that the induced magnetic field generated by the conductive shell of conductivity σ at a given instant t is equal to the induced magnetic field generated by a perfectly conductive moon at an earlier instant $t - \phi/\omega$ and multiplied by a constant A. It can be shown that for $\sigma < \infty$, the factor A given by **Equations 1.7** and **1.8** is always smaller than the perfect conductor value of $(r_0/r_m)^3$ and that the induced field would always lag behind the primary field, such that:

$$0 \leq A < \left(\frac{r_0}{r_m}\right)^3$$

$$0^\circ < \phi \leq 90^\circ$$

Analysing the limit cases for this solution in further detail, we can see that for the case of a perfectly conductive moon, where $r_1 = 0 \wedge r_0 = r_m$, we get $A = (r_0/r_m)^3 = 1$ and $\phi = 0$ using **Equations 1.7** and **1.8** once again. This correctly returns that the induced field response would be the same as the one given by a perfectly conductive moon, since $\mathbf{B}_{\text{sec}}(t) = \mathbf{B}_{\text{sec},\infty}(t)$. On the other hand, if we now consider the second extreme scenario, where we have a shell with a low conductivity ($\sigma \ll 1$), we see that A approaches zero. The same occurs if we have the conductive shell deep within the moon's interior ($r_0 \ll r_m$). In both these cases, the secondary field generated by the moon would be negligible and so the only contribution towards the total magnetic field measured would be the primary field. Lastly, from **Equations 1.7** and **1.8** we can see that A and ϕ only depend on r_0/r_m, $r_0 k$ and $r_1 k$. We can then introduce the skin depth $s = \sqrt{\mu_0\sigma\omega/2}$, which corresponds

to the penetration distance of a varying magnetic field into a semi-infinite conductor of conductivity σ, such that these quantities can alternatively depend on r_0/r_m, r_0/s and r_1/s. If we now consider the case in which the skin depth is equal to the moon radius ($s = r_m$), such that the magnetic field is able to penetrate the entire moon's interior, we can also define a reference conductivity $\sigma_m = 2/(\mu_0 \omega r_m^2)$ and use the quantities h and d as shown in **Figure 1.6** to describe A and ϕ.

We can then use real measurement data taken by spacecrafts during flybys to help constrain these parameters and thus indirectly determine these properties of the subsurface ocean layer. In [16], a deep analysis is made into the degenerate nature of the solutions we are able to obtain using this method, as different combinations of layer thickness h, layer depth d and conductivity can produced similar induced magnetic field responses. Although we won't be focusing on the study of these two moon's in particular, we will be using a similar methodology to study another of Jupiter's moons, Ganymede.

1.2.3 Ganymede

Aside from the intrinsic magnetic field generated in Ganymede's core, just like Europa and Callisto [16], there is also evidence for an induced dipole magnetic field in Ganymede [1] produced due to the interaction of Jupiter's time varying magnetic field with a conductive subsurface ocean layer, via Faraday's law. As such, the rotation of Jupiter's tilted magnetic moment results in a time varying magnetic flux at the position of Ganymede, giving rise to electric currents in the ocean layer that in turn generate the induced dipole magnetic field. This induced field can be used, just like we showed for the cases of Europa and Callisto, to extract valuable information about a moon's interior, since it is heavily influenced by the conductive properties of its composing materials. A perfect conductor would respond to the driving field, in this case, mainly in the Jupiter-Ganymede direction as shown in [1], by producing an induced field with equal magnitude and opposite direction, perfectly cancelling the driving field in the moon's interior. However, the magnetic field produced above Ganymede's surface would be the same as the exterior field produced by a uniformly magnetised sphere, which is nothing more then a magnetic dipole whose moment is oriented along the Jupiter-Ganymede direction, once again described in [1]. We can determine the moment of this dipole by requiring continuity of the normal component between the moon's interior and exterior.

1.3 JUICE

The JUICE (Jupiter Icy moon Explorer) spacecraft [20], which is scheduled to launch on an Ariane 5 rocket in September 2023, aims to analyse the Jovian system and evaluate the habitability of its moons, focusing on the study of Ganymede, Europa and Callisto. The possibility of a life-sustaining subsurface ocean on these three moons makes them prime targets not only for the search of microbial life in other bodies of the Solar System, but a potential emergence of life in Jupiter-like exoplanetary systems. Furthermore, JUICE will also allow us to study the overarching magnetic environment felt at different locations within the Jovian system.

1.3.1 Mission objectives

The spacecraft will resort to measurements of their sub-surfaces, surfaces, atmospheres and interactions with Jupiter's magnetosphere in order to fulfil the scientific goals of the

mission [20]:

Ganymede / Callisto

- characterisation of the ocean layers and detection of putative subsurface water reservoirs;
- topographical, geological and compositional mapping of the surface;
- study of the physical properties of the icy crusts;
- characterisation of the internal mass distribution, dynamics and evolution of the interiors;
- investigation of the exosphere;
- study of Ganymede's intrinsic magnetic field and its interactions with the Jovian magnetosphere.

Europa

- understanding the formation of its surface feature;
- study the chemistry essential to life.

After several flybys on both Europa and Callisto, the spacecraft will enter the final stage of its mission, as a dedicated orbiter of Ganymede, marking the first time a spacecraft orbits a moon other than Earth's.

1.3.2 Spacecraft trajectory

As previously mentioned, during the later portions its mission, JUICE will become a dedicated orbiter of Ganymede. This transition will be made gradually, with the spacecraft being assigned two distinct precessing circular orbits over the course of its study of Ganymede. As such, the spacecraft will provide a good coverage of Ganymede's entire surface during both orbital configurations. The first orbit corresponds to a precessing circular orbit with $r \sim 2.95\,R_G$ and a precession period of ~ 3 and a half days. The spacecraft's orbital path lines for this particular orbit are represented in **Figure 1.7**. During this stage of the mission, given that the spacecraft is far enough from Ganymede's surface, JUICE will be able to study the impact of Jupiter's magnetic field in the total magnetic field felt in this region of the near-Ganymede space. It will also be at this stage where possible compressions/expansions of Jupiter's magnetosphere might be detected using the spacecraft's magnetometers, as we will discuss further on. The spacecraft is expected to be in this orbital configuration for a duration of approximately 30 days.

Then, the spacecraft will perform several orbital transfer manoeuvres to move it into a lower circular orbit with a radius of $r \sim 1.185\,R_G$, or $\sim 487\,\text{km}$ above its surface. The precession period for this orbit is ~ 7.3 days. The spacecraft's orbital path lines for the second orbital configuration are represented in **Figure 1.8**. At this stage, JUICE will allows to study in great detail Ganymede's intrinsic and induced magnetic fields, as they have a stronger intensity near the surface. As such, it is at this stage where we can better characterise Ganymede's subsurface ocean layer. The spacecraft is expected to be in this orbital configuration for a duration of approximately 90 days.

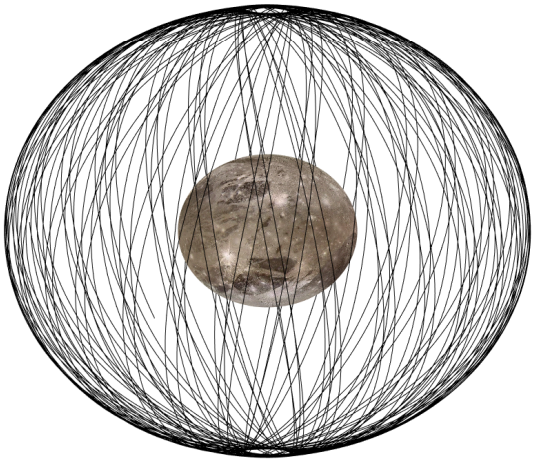

Figure 1.7: Orbital path lines for the first orbit type of the JUICE spacecraft around Ganymede. The mean orbital radius is $r \sim 2.95\,R_G$ and the precession period of the orbit is ~ 3.5 days.

(a) Orbital path lines after 15 days.

(b) Orbital path lines after 90 days. Here we clearly see the resulting full coverage of Ganymede's surface

Figure 1.8: Orbital path lines for the second orbit type of the JUICE spacecraft around Ganymede. The mean orbital radius is $r \sim 1.185\,R_G$ and the precession period of the orbit is ~ 7.3 days.

1.3.3 The J-MAG magnetometer

The JUICE Magnetometer (J-MAG) is one of the many instruments aboard the JUICE spacecraft to study the Jupiter-Ganymede environment. Its objective is to characterise the Jupiter's magnetic field, its interaction with Ganymede's own intrinsic and induced dipole fields and most notably determine the properties of a subsurface ocean in Europa, Callisto and Ganymede [20][21][22]. More precisely, this instrument will be able to measure the DC magnetic field vector at the spacecraft's location. In order to do that, J-MAG is located in

the spacecraft's 10.5 meter boom (**Figure 1.9**) and is composed of three main components: an inbound (MAGIBS) and one outbound (MAGOBS) 3-axis fluxgate magnetometers and a dark state scalar magnetometer (**Figure 1.10**). The use of two fluxgate magnetometers, in a so called dual fluxgate design, allows for a much better calibration of the data and provide redundancy in case one of these instruments fails to operate correctly. This improved calibration allows us to remove potential magnetic interference coming from the spacecraft's own electronic modules, as since the two fluxgate magnetometers are mounted at opposite ends of the giant boom, any noise caused by the electronics can be extracted from the actual measurement data using the gradiometer technique. This technique is based on the principle that the outbound fluxgate would be further away from the spacecraft's electronic modules and thus be less affected by any potential interference when compared to the inbound fluxgate, situated much closer to the body of the spacecraft. A detailed explanation on this technique is given in [23]. Since this offset in the data would take the form of a coherent and slowly varying DC field, it can be easily extracted from the data using this technique, not requiring any added roll procedures by the spacecraft to correct it.

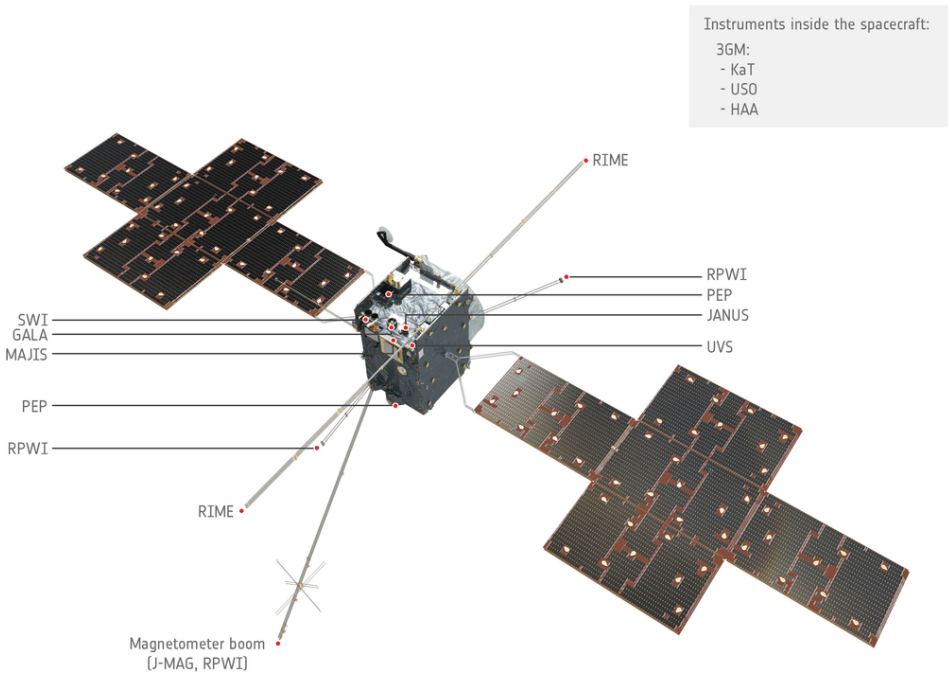

Figure 1.9: JUICE spacecraft and its instruments [24].

MAGOBS is composed of two orthogonal Permalloy ring-cores, each enabling us to measure the magnetic field in two axes across the plane of the ring, while MAGIBS possesses two orthogonal ring-cores that allow for the measurement of the magnetic field across one axis each and a coil for the measurement of the third axis [22]. With such a setup, both fluxgate magnetometers allow us to accurately determine the three-dimensional vector of the total magnetic field at the spacecraft's position, having such a system been previously used in missions such as Cassini and THEMIS [20]. As for the scalar magnetometer, MAGSCA, it will be mounted at the very tip of the boom, with its function being to determine with much higher precision the magnitude of the measured

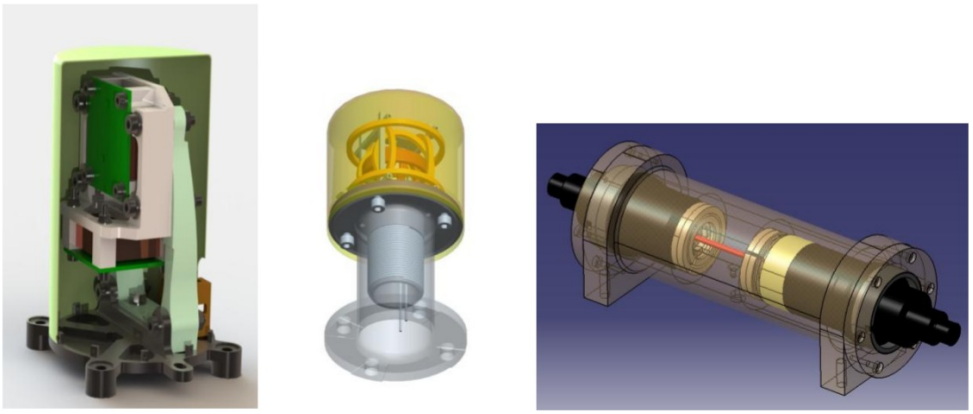

Figure 1.10: The three components of J-MAG, MAGIBS (left), MAGOBS (centre) and MAGSCA (right) [20].

magnetic field, rather than its direction [21]. Both fluxgate magnetometers possess two operating measurement ranges of $\pm 8\,\mu T$ and $\pm 50\,\mu T$, with a precision value of $\pm 1\,pT$ and $\pm 6\,pT$ for the two ranges, respectively. This dual-system allows the system to correctly adapt to the optimal measurement range based on the incoming magnetic field signal. As for the scalar magnetometer, its nominal measurement range is $0 - 50\,000\,nT$ with a precision of $3\,pT$ [22]. J-MAG's maximum inherent noise performance is $10\,pT/\sqrt{Hz}$, giving it a high sensitivity capable of comfortably satisfying all of its scientific requirements. Further details J-MAG's characteristics are present in **Table 1.1**. The instrument's noise performance and resolution will be of particular interest to our work as we shall discuss in the next section.

Table 1.1: J-MAG performance characteristics [20].

Parameter	Units	Value
Instrument noise performance	$pT/\sqrt{Hz}$	< 10 (at 1 Hz)
MAGOBS/IBS orthogonality (calibrated)	°	$< 0.01°$
Offset stability (fluxgate)	nT/hour	< 0.5nT/100 hours
Offset stability (scalar)	nT	< 0.1
Linearity	%	< 0.05
Operating temperature range for MAGOBS/IBS/SCA sensors	°C	-75 to $+60$(TBC)
Survival temperature range for MAGOBS/IBS/SCA (measured at the MAG T_{SENS})	°C	-150 to $+80$(TBC)
Measurement ranges (MAGOBS/IBS operational)	nT	$\pm 8000, \pm 50000$
Bits per field component	N/A	20
Resolution (MAGOBS/IBS ranges)	pT	1, 6
Resolution (MAGSCA)	pT	10

1.3.3.1 Using J-MAG to detect changes in Jupiter's magnetosphere

As we have discussed before, one aspect to take into account when analysing the Jovian magnetic field is the possible compression and expansion of its magnetosphere due to the interaction with solar wind. By impacting the overall shape of Jupiter's magnetosphere, one would also expect to also see variations on the strength and direction of the magnetodisk field. The impact of these changes on the plasma flow and on the

overarching magnetic field is another area that requires further study. These variations may very well be detectable using J-MAG if they fall above the instrument's sensitivity, and so we may also use it to gain insight into this intricate mechanism. In order to study this possibility, we will use data files that allows us to compute the magnetodisk field resulting of different magnetosphere configurations. We will then use our magnetic field model to determine the expected variations and determine if these will be detectable by the spacecraft. For this will use Gaussian noise in order to simulate the natural noise coming from the various electronics modules and other external sources that may affect J-MAG's measurements. In the case that these variations are indeed detectable by this instrument, we can then estimate the maximum Gaussian noise standard deviation value for each we lose the necessary sensitivity to do so. In order to do so, we can use **Equation 1.11** to quantify, for a given standard deviation value σ, how sensitive the instrument will be to those variations:

$$\Delta = \overline{|\delta|} - \sqrt{\frac{1}{n}\sum_{i}\left(\delta_{\mu} - \delta_{\sigma}\right)^{2}} \tag{1.11}$$

where Δ corresponds to the sensitivity of the magnetometer to the signal, $\overline{|\delta|}$ to an approximate magnitude of the variations, n the number of data points, δ_{μ} the variation predicted by the model with no noise and δ_{σ} the predicted variation with Gaussian noise added. By definition, the value of Δ should be positive for a noiseless measurement and decrease as we add noise with greater standard deviations, becoming negative once the overall noise intensity surpasses that of the signal.

Chapter 2

Project's aim and preliminary results

While JUICE will not reach its destination - Jupiter - until around 2030, now is the time for us to start making predictions about the types of in situ measurements that the spacecraft will make when it enters its final mission phase as a dedicated orbiter of Ganymede. As such, this MSc project will focus on the development of a comprehensive magnetic field model of the Jupiter Ganymede system and use it to predict the JUICE magnetometer measurements in the near-Ganymede space. The developed model will include contributions of the ambient Jovian magnetodisk field, Ganymede's intrinsic and induced field. As mentioned before, we will also try to determine if variations in the overall shape of Jupiter's magnetosphere, due to its interaction solar wind and CMEs, could be detected using JUICE's magnetometer, J-MAG. Furthermore, the final model could also be expanded upon, in order to try model the plasma currents that flow within Jupiter's magnetosphere, and how these could further impact our results. In this chapter, we will present a brief overview of the methodology we are currently using to achieve these objectives and show some of the preliminary results we have obtained so far.

2.1 Analysis of the field contributions in the near-Ganymede space

2.1.1 Jupiter's magnetodisk field

Using a previously developed function to model Jupiter's magnetodisk field we were able to analyse its influence on the overall magnetic field felt by a spacecraft at different positions in the near-Ganymede space. Since we are mostly interested in studying the magnetic field variations at distances no greater than 10 R_G from its centre, we can approximate this field contribution as a uniform magnetic field, orientated along a 40.1° angle in relation to the Jupiter-Ganymede direction, and varying only due to the rotation of Jupiter's tilted magnetic moment. **Figure 2.1** illustrates the change in strength of the different field components due to this change in the phase of its magnetic moment.

2.1.1.1 Ganymede's internal field

We then modelled the intrinsic dipole field of Ganymede and analysed its variation at different spatial positions from Ganymede's centre, as well as the strength of the field components for spherical surfaces, with different radii, centred on Ganymede. By doing so, we observed that Ganymede's intrinsic magnetic field has a dominant role in the overarching field felt at its surface and the inner regions of its own small magnetosphere. We also determined that this field is stronger near the polar regions, where there exists

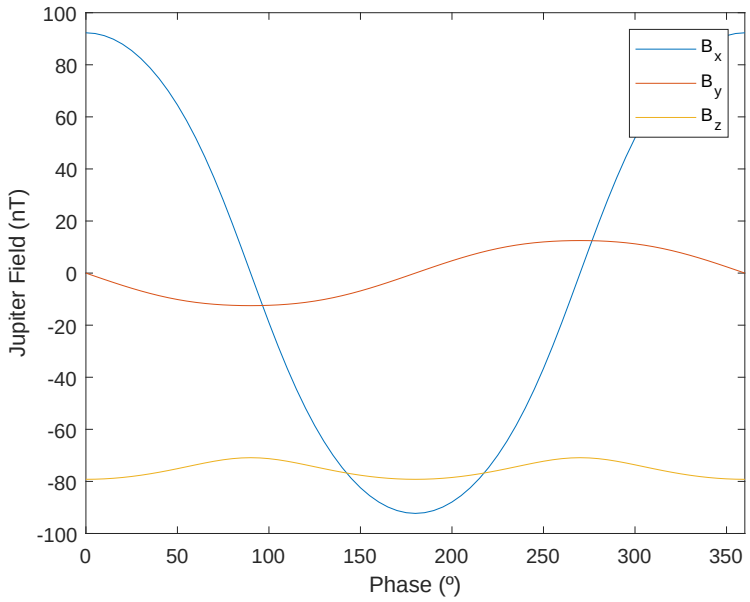

Figure 2.1: Field strength variation due to Jupiter's rotation. Phase 0 corresponds to Jupiter's magnetic moment pointing towards Ganymede. Furthermore, the x-component corresponds to the Jupiter-Ganymede direction, y to a perpendicular direction within the orbital and z to the normal direction to that very same plane.

a higher concentration of field lines. Lastly, we concluded that the overall field strength decreases rapidly as we move away from Ganymede's surface, becoming negligible ($< 1\,\text{nT}$) for distances greater than $10\,R_G$.

2.1.2 Induced dipole field and total magnetic field

The induced dipole field component was then added to the model using the approach described in **Section 1.2.3**, finalising its development. With this, we are able to determine the total magnetic field direction and magnitude at a given point in space around Ganymede. As such, we analysed the total field for the same spherical surfaces centred on Ganymede. We also conducted the same analysis for different phases of Jupiter's magnetic moment (**Figure 2.2**). We concluded that at these distances, the x-component of the field, whose orientation falls on the Jupiter-Ganymede direction, is dominant whilst the y-component is almost negligible when compared to the rest.

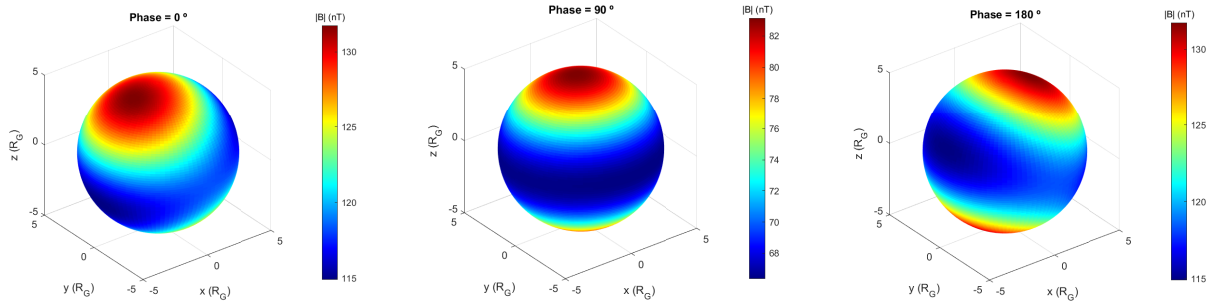

Figure 2.2: Spherical plots, with $r = 5\,R_G$, of the total field's magnitude for Jupiter's magnetic moment phase 0° (left), 90° (middle) and 180° (right).

In order to better evaluate the impact of each contributor to the overarching field, we

then analysed the percentile contribution and angle relation between each one of them at different radial distances and magnetic moment phases (**Figure 2.3**). We can observe that Ganymede's intrinsic field affects mostly the polar regions of the moon, despite the moon having two circular regions around the poles where this field has no contribution to the total field.

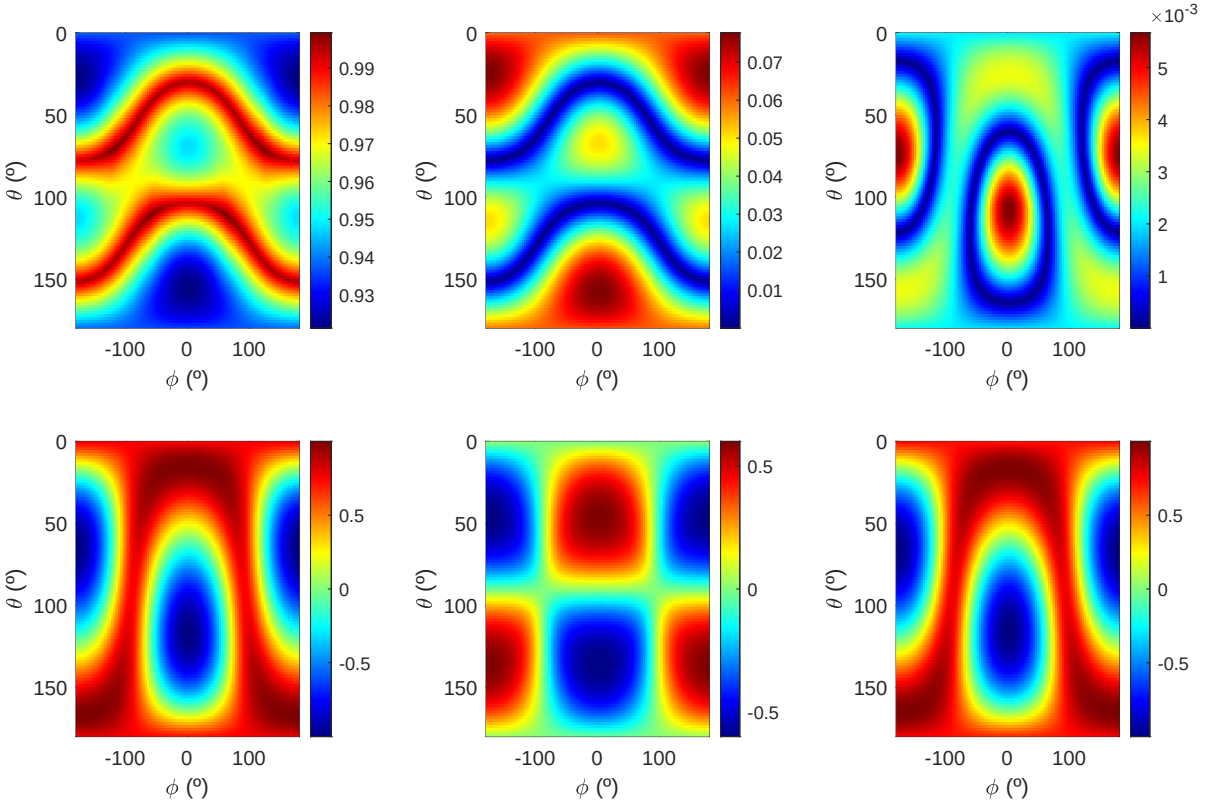

Figure 2.3: Percentile contributions of Jupiter's magnetodisk field (top-left), Ganymede's internal field (top-middle) and induced dipole field (top-right) towards the total magnetic field at $r = 5\,R_G$. The cosine of the angle between the total field and the different contributors is also shown (bottom row).

2.2 Sensitivity to the compression/expansion of Jupiter's magnetosphere

Having developed and analysed the main results that can be extracted from the magnetic field model, we proceeded to use it in order to determine if the on-board magnetometer, J-MAG, would be sensitive to the variations in the magnetodisk field caused by a compression/expansion of Jupiter's magnetosphere. We analysed two different magnetosphere configurations and using the model we determined the total field detected by a spacecraft in circular orbits, with varying radii, around Ganymede. Gaussian noise was also added to the result of the expected total field for each configuration in order to simulate the real data obtained from the magnetometer. The results for each expected total field component were then subtracted between both configurations in order to obtain the change detectable by the spacecraft in that circular orbit (**Figure 2.4**).

We then used **Equation 1.11** to determine the maximum standard deviation value after which the instrument can no longer reliably detect the variations in Jupiter's magnetosphere (**Figure 2.5**).

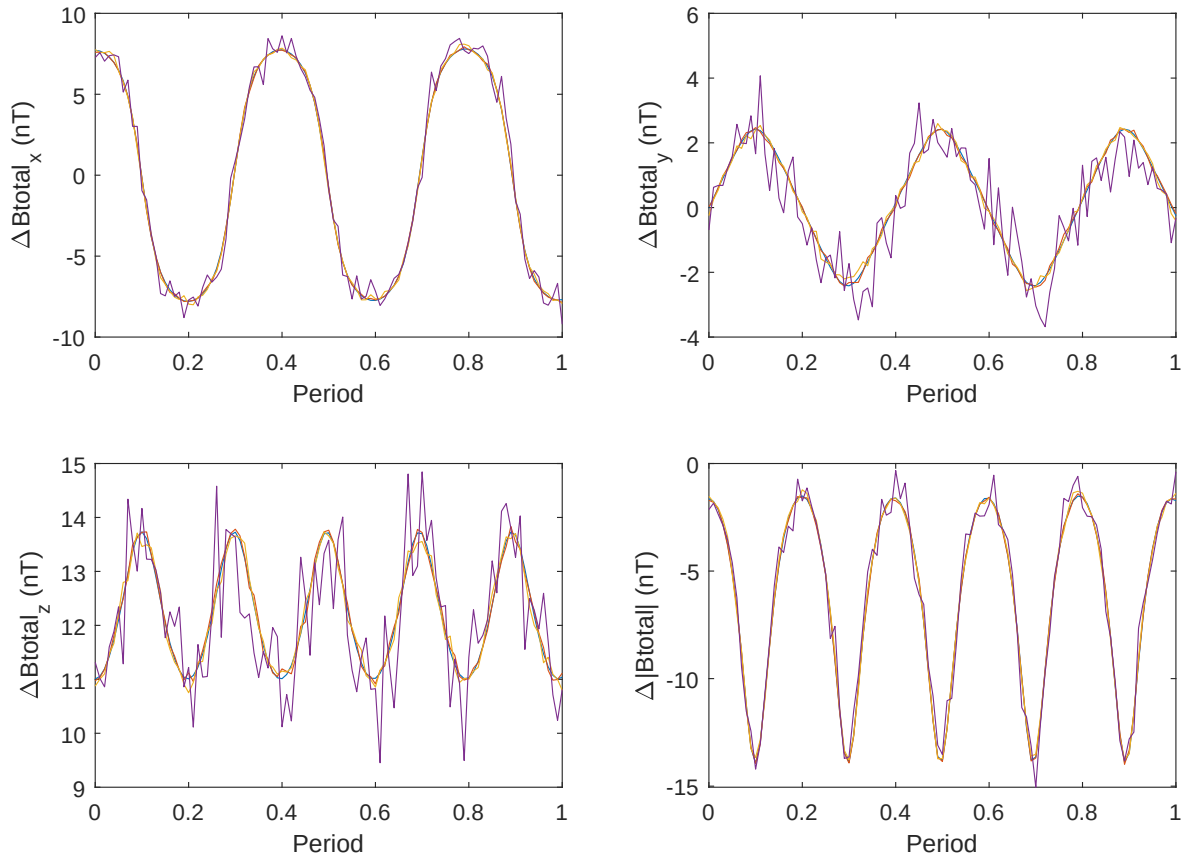

Figure 2.4: Change in total magnetic field as observed by a spacecraft in a circular orbit, $r = 5\,R_G$, around Ganymede. The results were taken over one orbital period and shown for each component of the total field, as well as its magnitude. Different colour curves are shown for the expect result (blue) and for a varying value of Gaussian noise standard deviation: $\sigma = 0.05\,\text{nT}$ (red), $\sigma = 0.1\,\text{nT}$ (yellow) and $\sigma = 0.5\,\text{nT}$ (purple).

A better way to look at these results is dividing them by the standard deviation value itself, giving us an equivalent to the sigma p-value evaluation method commonly used in particle physics. Using this approach, we determined that in order to detect compression/expansion of Jupiter's magnetosphere in at least one of the total field components, with a confidence value of 5 σ, we must have $\sigma < 1.9\,\text{nT}$. From **Figure 1.1**, we can see that this is well within MAGOBS, MAGIBS and MAGSCA's capabilities. However, if we want to measure the variations in all components we must heavily restrict the standard deviation value of the noise to $\sigma < 0.22\,\text{nT}$, which despite being fairly more demanding, would still be comfortably within J-MAG's detection range. As such, these results show that it should be possible to detect the compression/expansion of Jupiter's magnetosphere using J-MAG measurements.

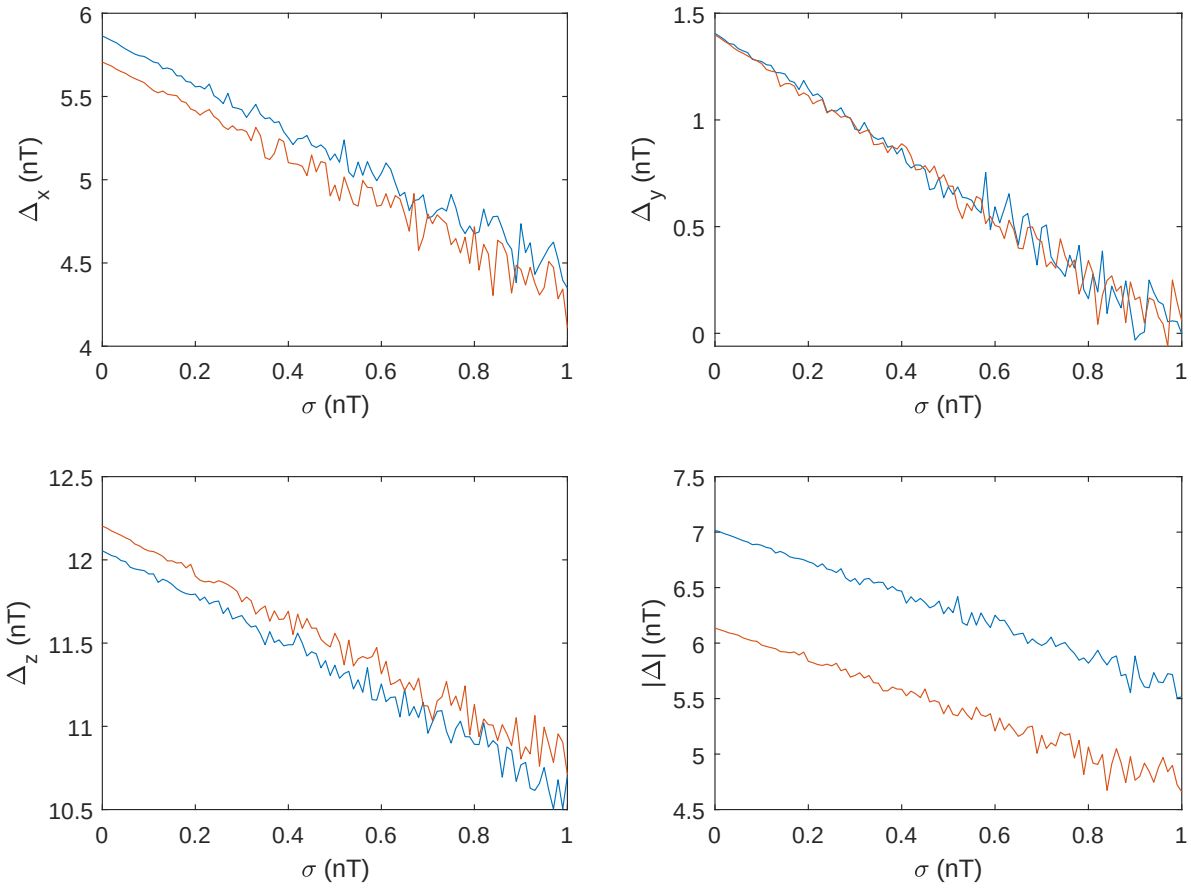

Figure 2.5: Sensitivity of the magnetometer to the variations in Jupiter's magnetosphere for different Gaussian noise intensities. The results show the behaviour for orbits with $r = 2\,R_G$ (blue) and $r = 5\,R_G$ (orange). We can see that the instrument is able to detect significant variations in both the x and z components of the total field, while the y component variations can be only detectable for a small standard deviation value.

Chapter 3

Conclusion and future work

In this essay we presented some of the major contributions and processes that result in the complex magnetospheric structures we observe in the Jovian system and how one can use computational models, allied with in situ magnetic field measurements, to characterise the magnetic environment and probe the inner composition of planetary bodies. The interactions between Ganymede's own intrinsic and induced magnetic field with the ambient Jupiter field still leave many questions unanswered, as the importance of the different magnetic field contributions to the total field is still not fully understood. As we saw, others factors such as compressions/expansions of Jupiter's magnetosphere and the importance of plasma flow to this overarching magnetic field of the system add to the complexity of this problem. However, using the methodology described in this essay we hope not only to determine the impact of each one of these contributions but also expand on the work done by [1], analysing the nature of Ganymede's interior and setting constrains on the depth, width and conductive properties of its subsurface ocean layer, based on the results of our magnetic field model.

In the near future, we will focus on predicting the magnetic field data collected by the JUICE spacecraft in its two orbital configurations around Ganymede and developing a robust fitting model for this data, in order to extract the properties of its ocean layer. We will also check how effectively different harmonics of the field oscillation can be picked up by Fourier analysis. To do so, we will analyse the influence of noise, which could be additional real fluctuations in the field due to various plasma currents, on the accuracy with which the power in the higher harmonics can be estimated by J-MAG. This will ultimately allow us to check the performance of our model, by comparing it with future real JUICE measurements, and estimate the impact of the plasma currents on the different other contributions to the total magnetic field. Furthermore, an in-depth analysis of the magnetic reconnection processes that continuously occur due to the Jupiter-Ganymede magnetospheric interaction could be made in the future, utilising our model and in-situ measurements taken by JUICE and other future spacecrafts. Lastly, a study on the overall plasma flow could also be conducted by incorporating some of the contributions from other moons of Jupiter into our model in order to create a more general model, not restricted to the near-Ganymede space, and get a better understanding of their importance to the flow of charged particles across the Jovian system.

Bibliography

[1] M.G. Kivelson, K.K. Khurana and M. Volwerk. "The permanent and inductive magnetic moments of ganymede". In: *Icarus* 157.2 (2002), pp. 507–522. DOI: 10.1006/icar.2002.6834.

[2] B. Steigerwald. *Voyager enters Solar System's final frontier*. 2005. URL: https://www.nasa.gov/vision/universe/solarsystem/voyager_agu.html (visited on 24/03/2022).

[3] *Voyager Probes Heliosphere Chart*. URL: https://www.jpl.nasa.gov/images/pia22566-voyager-probes-heliosphere-chart (visited on 24/03/2022).

[4] E. N. Parker. *Dynamics of the interplanetary gas and magnetic fields*. URL: https://ui.adsabs.harvard.edu/abs/1958ApJ...128..664P/abstract (visited on 24/03/2022).

[5] Alan Hood. *Parker's Solar Wind Model*. URL: http://www-solar.mcs.st-andrews.ac.uk/~alan/sun_course/Chapter6/node3.html (visited on 24/03/2022).

[6] B.M. Jakosky et al. "Loss of the martian atmosphere to space: Present-day loss rates determined from Maven observations and integrated loss through time". In: *Icarus* 315 (2018), pp. 146–157. DOI: 10.1016/j.icarus.2018.05.030.

[7] M. Opher. "The heliosphere: What did we learn in recent years and the current challenges". In: *Space Science Reviews* 200.1-4 (2015), pp. 475–494. DOI: 10.1007/s11214-015-0186-3.

[8] N. Achilleos. "The nature of Jupiter's Magnetodisk current system". In: *Electric Currents in Geospace and Beyond* (2018), pp. 127–138. DOI: 10.1002/9781119324522.ch8.

[9] Joachim Saur et al. "Plasma interaction of Io with its plasma torus". In: *Jupiter. The Planet, Satellites and Magnetosphere* (Jan. 2004).

[10] Kenneth R. Lang. *Flux tube and plasma torus*. URL: https://ase.tufts.edu/cosmos/view_picture.asp?id=718 (visited on 24/03/2022).

[11] Cowley et al. "Reconnection in a rotation-dominated magnetosphere and its relation to Saturn's auroral dynamics". In: *JOURNAL OF GEOPHYSICAL RESEARCH* 110 (2005). DOI: 0.1029/2004JA010796.

[12] S. V. Badman and S. H. Cowley. "Significance of Dungey-cycle flows in Jupiter's and Saturn's magnetospheres, and their identification on closed equatorial field lines". In: (). URL: https://angeo.copernicus.org/articles/25/941/2007/ (visited on 24/03/2022).

[13] E. Chané et al. "How is the Jovian main auroral emission affected by the solar wind?" In: *Journal of Geophysical Research: Space Physics* 122.2 (2017), pp. 1960–1978. DOI: 10.1002/2016ja023318.

[14] E. Chané, J. Saur and S. Poedts. "Modeling Jupiter's magnetosphere: Influence of the internal sources". In: *Journal of Geophysical Research: Space Physics* 118.5 (2013), pp. 2157–2172. DOI: 10.1002/jgra.50258.

[15] K. J. Trattner, S. M. Petrinec and S. A. Fuselier. "The location of magnetic reconnection at Earth's magnetopause". In: *Space Science Reviews* 217.3 (2021). DOI: 10.1007/s11214-021-00817-8.

[16] C Zimmer. "Subsurface Oceans on Europa and callisto: Constraints from Galileo magnetometer observations". In: *Icarus* 147.2 (2000), pp. 329–347. DOI: 10.1006/icar.2000.6456.

[17] Jodi R. Berdis et al. "Europa's surface water ice crystallinity: Discrepancy between observations and Thermophysical and particle flux modeling". In: *Icarus* 341 (2020), p. 113660. DOI: 10.1016/j.icarus.2020.113660.

[18] W. B. Sparks et al. "Active cryovolcanism on Europa?" In: *The Astrophysical Journal* 839.2 (2017). DOI: 10.3847/2041-8213/aa67f8.

[19] W. Parkinson. In: *Introduction to geomagnetism*. Scottish Academicpress, 1983, pp. 308–340.

[20] European Space Agency. *JUICE*. URL: https://sci.esa.int/web/juice/-/50068-science-objectives.

[21] Austrian Academy of Science. URL: https://www.oeaw.ac.at/en/iwf/research/space-missions/future-missions/juice/magsca (visited on 24/03/2022).

[22] National Aeronautics and Space Administration (NASA). *NASA Space Science Data Coordinated Archive - JUICE Magnetometer (J-MAG)*. URL: https://nssdc.gsfc.nasa.gov/nmc/experiment/display.action?id=JUICE++++-07 (visited on 24/03/2022).

[23] Ovidiu Dragoş Constantinescu et al. "Principal component gradiometer technique for removal ofspacecraft-generated disturbances from magnetic field data". In: (2020). DOI: 10.5194/gi-2020-10.

[24] *JUICE's Instruments*. URL: https://sci.esa.int/web/juice/-/61110-juice-instruments (visited on 24/03/2022).

[25] Nicholas Achilleos et al. "The magnetodisk regions of Jupiter and Saturn". In: *Magnetospheres in the Solar System* (2021), pp. 453–469. DOI: 10.1002/9781119815624.ch29.

[26] European Space Agency. *JUICE Definition Study Report (Red Book)*. 2014.

[27] N. Krupp et al. "Dynamics of the Jovian magnetosphere". In: *Jupiter. The Planet, Satellites and Magnetosphere*. Ed. by Fran Bagenal, Timothy E. Dowling and William B. McKinnon. Vol. 1. 2004, pp. 617–638.